Science of Sintering, **53** (2021) 1-8

https://doi.org/10.2298/SOS2101001F

UDK: 553.689; 692.533.1; 622.785

Multiferroic Heterostructure $BaTiO_3/\varepsilon$-Fe_2O_3 Composite Obtained by *in situ* Reaction

S. Filipović[1*)], N. Obradović[1], Lj. Andjelković[2], D. Olćan[3], J. Petrović[3], M. Mirković[4], V. Pavlović[5], D. Jeremić[6], B. Vlahović[7], A. Đorđević[3,8]

[1]Institute of Technical Sciences of the Serbian Academy of Sciences and Arts, Belgrade, Serbia

[2]University of Belgrade–Institute of Chemistry, Technology and Metallurgy, Department of Chemistry, Njegoševa 12, 11000 Belgrade, Serbia

[3]University of Belgrade – School of Electrical Engineering, Belgrade, Serbia

[4]Department of Materials, „VINČA" Institute of Nuclear Sciences - National Institute of the Republic of Serbia, University of Belgrade, Belgrade, Serbia

[5]University of Belgrade – Faculty of Agriculture, Belgrade, Serbia

[6]Innovative Centre of the Faculty of Chemistry, University of Belgrade, StudentskiTrg 12-16, Belgrade, Serbia

[7]North Carolina Central University, Durham, NC, USA

[8]Serbian Academy of Sciences and Arts, Belgrade, Serbia

Abstract:

Solid-state reaction between $BaTiO_3$ and Fe_2O_3 was used to produce a multiferroic heterostructure composite. Commercial $BaTiO_3$ and $Fe(NO_3)_3 \cdot 9H_2O$ were suspended in ethanol for 30 minutes in an ultrasound bath. The prepared mixture was thermally processed at 300 °C for 6 h. Sintering at 1300 °C for 1 h resulted in a mixture of different phases, $BaTiO_3$, $BaFe_{12}O_{19}$ and $Ba_{12}Ti_{28}Fe_{15}O_{84}$, which were confirmed by x-ray powder diffraction. A dense microstructure with a small volume fraction of closed porosity was indicated by the scanning electron microscopy, while a homogeneous distribution of Fe ions over $BaTiO_3$ phase was visible from energy dispersive spectroscopy mapping. Doping of $BaTiO_3$ with Fe_2O_3 resulted in formation of magnetic hexaferrite phases, as confirmed by dielectric measurements that showed a broadened maximum of the permittivity measured as a function of temperature.

***Keywords**: $BaTiO_3$; Composite; Multiferroic; Solid-State Reaction; Sintering.*

1. Introduction

Magnetoelectric multiferroics have recently attracted great attention due to their extraordinary properties [1]. Magnetoelectric multiferroic composites possess magnetic and ferroelectric order simultaneously. The electrical properties of these materials are affected by applying a magnetic field and vice versa [2]. Single phase materials, i.e. compounds that exhibit two or more ferroic order phenomena in the same phase are scarse and there are only few known compounds with functional electric and magnetic properties especially close to room temperature. To overcome the rareness and shortcomings of single phase magnetoelectrics, many magnetoelectric multiferroic composites were developed. The

*) **Corresponding author:** suzana.filipovic@itn.sanu.ac.rs (Dr. Suzana Filipović)

magnetoelectric coupling, in these materials, is a consequence of the strain induced on the interface between two different phases [3]. The final properties of such heterostructured materials can be adjusted by varying the microstructure of the constituents, their volume fraction, and/or the phase composition. Their diverse functional properties enable their application in different devices, such as multi-state memory elements, transducers, wireless communication and, recently, as materials for photocatalysis [4-7].

$BaTiO_3$ is the most frequently used ferroelectric for designing magnetoelectric multiferroic materials [8-9]. Its frequent use is due to its structure and dielectric properties [10], [11]. The stable phases of $BaTiO_3$ are a paraelectric cubic structure and a ferroelectric tetragonal structure [12-13]. The ferroelectricity in the tetragonal phase originates from distortions of the crystal lattice and displacement of the Ti ions from the centre of the unit cell that induces permanent dipoles and ferroelectric behaviour. The transition from the tetragonal to the cubic phase occurs at 130 °C [14-16]. This transition can be detected by changes in the dielectric permittivity vs. temperature, as a sharp peak. The formation of the heterostructure composite material or doping of $BaTiO_3$ can broaden the maximum of the permittivity measured as a function of temperature.

Among comprehensive investigations of iron (III) oxide, this compound attracts the interest of researchers dedicated to design multiferroics, due to its specific magnetic properties [10], [17-19]. α-Fe_2O_3, hematite, is the most stable phase at room temperature and exhibits antiferromagnetic behaviour [20]. Maghemite, γ-Fe_2O_3, is a metastable phase, which transforms into α-Fe_2O_3 at approximatel 400 °C[21]. β-Fe_2O_3stable form occurs only in materials with nanosized dimensions. β-Fe_2O_3 is the only phase of iron oxides that shows paramagnetism at room temperature [22]. Recently, ε-Fe_2O_3 has been investigated because it possesses so-called "canted ferromagnetism properties" because of multiple possible magnetic interactions. The large distortions of the lattice network provide antiferromagnetic and ferromagnetic couplings. It is a very rare phase with scarce natural abundance, existing only as nanosized object. Furthermore, it is very difficult to obtain it as a single phase, and it is thermally unstable. However, its various application-promising properties, encompassing a giant coercive field at room temperature, significant ferromagnetic resonance, and coupled magnetoelectric features that are not observed in any other simple metal oxide phase, raised its intense research in the past years [23]. A large coercive field, approximately 1600 kA/m, makes it a candidate for magnetic recording and data storage [24-25].

Composite materials based on α-Fe_2O_3/$BaTiO_3$ appear in various forms, such as mixed powders that are subsequently sintered, core/shell particles, or various thick films that can be prepared by simple mixing of powders, sol-gel method, etc.[3], [8], [22]. Having in mind the interesting properties of the epsilon phase of Fe_2O_3, multiferroic composites based on ferroelectric $BaTiO_3$ and magnetic ε-Fe_2O_3 are worth being investigated, including their behaviour at elevated temperatures. In this paper, we have examined a $BaTiO_3$/ε-Fe_2O_3 composite obtained by *in-situ* preparation of ε-Fe_2O_3 in nanocrystalline form.

2. Materials and Experimental Procedures

Commercial $BaTiO_3$ (Sigma Aldrich) and $Fe(NO_3)_3 \cdot 9H_2O$ (Sigma Aldrich) were used. Suspension of 2.57 mmol (0.6 g) $BaTiO_3$ and 1.28 mmol (0.5 g) $Fe(NO_3)_3 \cdot 9H_2O$ in 100 ml ethanol was prepared, and treated for 30 minutes in an ultrasound bath. The solvent was evaporated at 50°C, and the prepared mixture was thermally processed in an electric furnace at 300 °C for 6 h.

The synthesized powder was pressed at 300 MPa using a uniaxial double- action pressing process with an 8 mm diameter tool (hydraulic press RING, P-14, VEB THURINGER). The compacted sample was sintered in air in a tube furnace (Protherm PTF 16/75/450) using the following temperature program: heating to 1300 °C at a rate of 10

°C/min, dwelling at 1300 °C for 1 h, and cooling to room temperature spontaneously. The sintered sample was denoted by BTF1300 according to the preparation conditions.

The morphology and composition of the BT, BTF and BTF1300 powders was determined by the scanning electron microscopy (SEM; JEOL JSM-6390 LV) coupled with electron dispersive spectroscopy (EDS; Oxford Instruments X-MaxN). The micrograph of sintered sample was recorded on the top of the crushed sample. As a part of the preparation process, samples were placed on a carbon tape and covered with gold for a conductive coating. The accelerating voltage in the SEM was in the range 20-30 kV.

The phase composition was characterized at room temperature by the X-ray powder diffraction (XRPD; Ultima IV Rigaku) equipped with $CuK\alpha_{1,2}$radiation, using a generator voltage of 40.0 kV and a generator current of 40.0 mA. The range of 10–90° 2θ was used with a scanning step size of 0.02° and at a scan rate of 5°/min, using D/TeX Ultra high - speed detector. A Si monocrystalline sample carrier was used. The PDXL2 (Ver. 2.8.4.0) software was used to evaluate the phase composition and identification. All obtained powders were identified using data from the ICDD data base[27], [28]. PDXL2 software was used for calculation of the microstructural parameters, and the results are shown in Tab. I.

Tab. I Summary of XRD analysis.

Phase name	ICDD PDF card number	Unit cell parameters							Microstructural parameters	
		a (Å)	*b* (Å)	*c* (Å)	*α* (°)	*β* (°)	*γ* (°)	*V* (Å^3)	crystallite size (nm)	strain (%)
$BaTiO_3$	01-075-1169	3.991(5)	3.991(5)	4.034(9)	90	90	90	64.28(18)	65.3(6)	2.95(9)
ε - Fe_2O_3	00-58-0266	5.096(11)	8.830(3)	9.150(7)	90	90	90	412(4)	14.9(14)	0.00(3)

The relative dielectric permittivity (dielectric constant) and the loss tangent of the sintered specimens were measured with a technique specially developed for characterization of ceramic materials. We have designed and manufactured a coaxial chamber and developed dedicated software, as described in our previous paper [29]. The reflection coefficient at the SubMiniature version A (SMA) connector of the chamber was measured using a vector network analyser (Agilent E5061A). From this coefficient, the input complex admittance of the chamber was calculated using numerical electromagnetic models. Within this experiment, the circular faces of the disc-shaped sample were covered with silver, and the measurement was performed in air, in the temperature range from room temperature to 170 °C. The measurement frequency was 5 MHz, and data were recorded during heating and cooling.

3. Results and Discussion

The XRPD pattern of the BTF synthesized sample is presented in Fig. 1.

Based on the XRPD results, $BaTiO_3$ was the main phase. Besides sharp and intense peaks of barium titanate, some other low intensity peaks of ε-Fe_2O_3 were also observed. The synthesis method led to formation of the orthorhombic ε-Fe_2O_3 phase. This phase is an intermediate product of transformation between the metastable beta and gamma phases. The epsilon phase has been the subject of many recent studies, due to its magneto-electric coupling, where the structural stability of ε-Fe_2O_3 strongly depends on its particle size [30].
The XRD analysis revealed that the size of the domain of coherent scattering of the synthesized ε-Fe_2O_3 was around 15 nm, with practically no measurable strain.

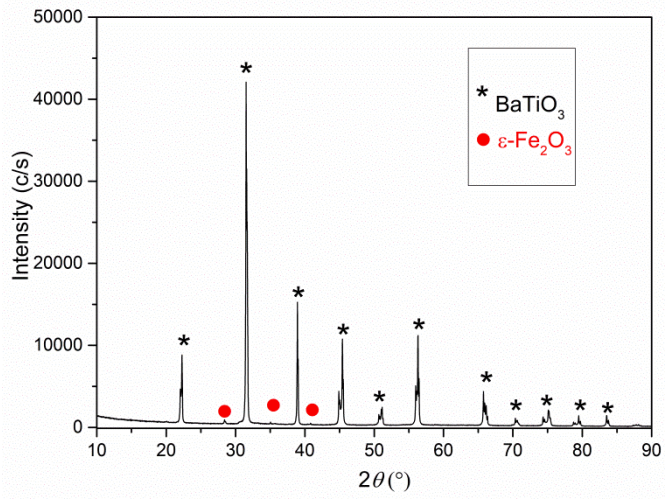

Fig. 1. XRD pattern of BTF.

Fig. 2. shows the SEM micrograph and EDS maps of the synthesized composite powder. The micrograph indicates polygon-shaped particles, less than 1 μm in diameter, uniformly distributed within the sample, without hard agglomerates. EDS mapping shows $BaTiO_3$ particles that are uniformly covered with Fe.

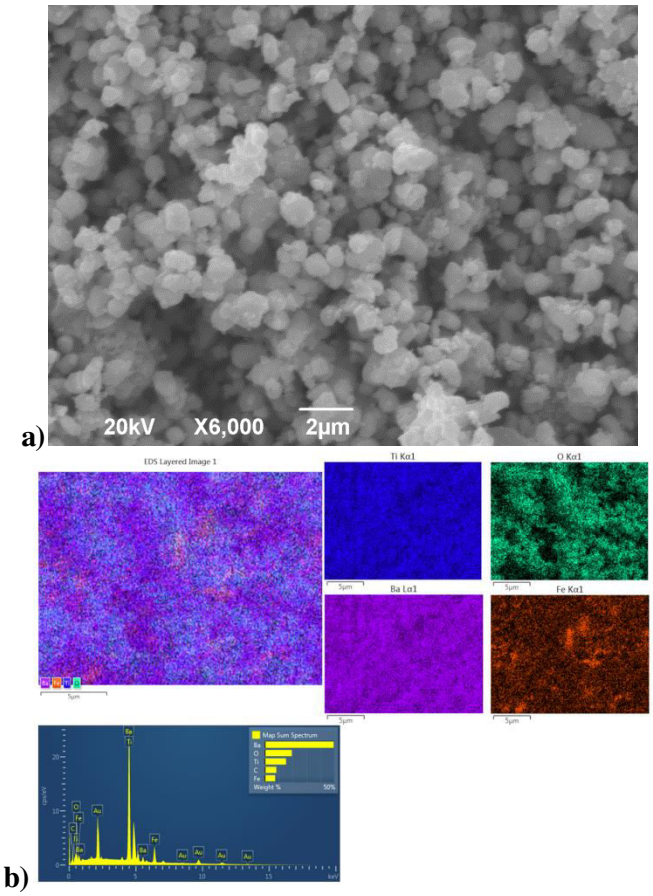

Fig. 2. a) SEM micrograph and b) EDS maps of the BTF composite.

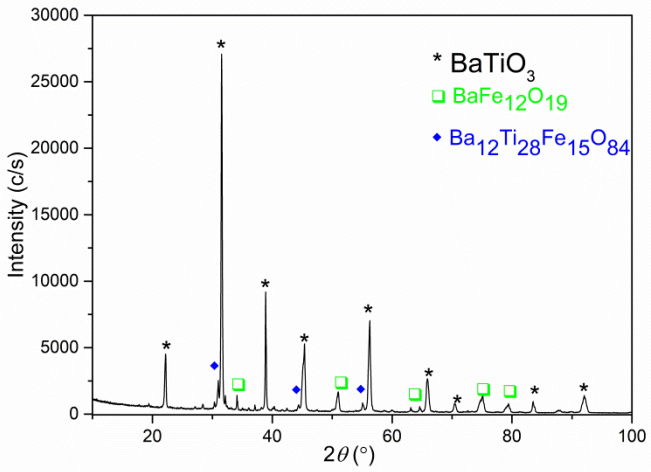

Fig. 3. XRD pattern of BFT1300.

The XRPD pattern of the sintered specimen is presented in Fig. 3 and shows that the main phase was $BaTiO_3$. The peaks of this phase are sharp and well defined, which can be related to good crystallinity. A low secondary peak belongs to the barium dodecaferrate (III) phase with a hexagonal crystal structure and $BaFe_{12}O_{19}$ with the $P6_3/mmc$ (194) space group (01-075-9113). Moreover, the presence of $Ba_{12}Ti_{28}Fe_{15}O_{84}$ was also revealed, as a complementary phase. These two phases occur together during sintering of $BaTiO_3$ and Fe_2O_3, on the interfaces in the multiferroic heterostructure composite.

Fig. 4. shows a SEM micrograph and EDS maps of the sintered specimen. The micrograph indicates that the final sintering stage was achieved, producing well sintered parts with very small closed pores that were less than 500 nm in diameter. The EDS maps of the sintered sample are consistent with the presence of the $BaTiO_3$ phase with equally distributed Fe ions.

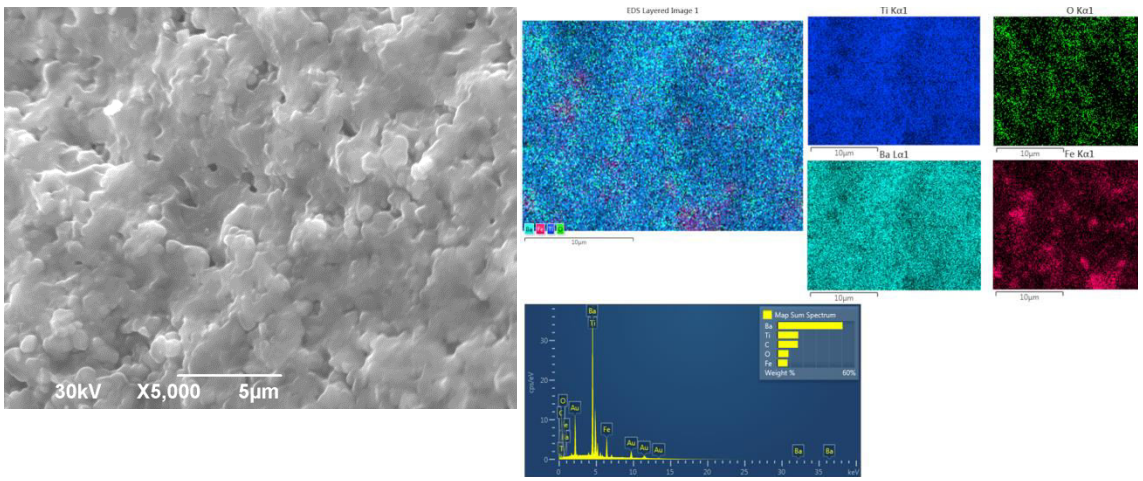

Fig. 4.a) SEM and b) EDS of BTF1300.

Fig. 5. shows the relative permittivity and loss tangent of BFT1300 as functions of the temperature. The relative permittivity is in the range from 1100 to 1700, reaching the maximum of 1700 at the temperature of the $BaTiO_3$ phase transition from tetragonal to cubic (130 °C). The broadened permittivity maximum is due to Fe doping of $BaTiO_3$ and the formation of magnetic hexaferrite phases ($BaFe_{12}O_{19}$ and $Ba_{12}Ti_{28}Fe_{15}O_{84}$) at the interface.

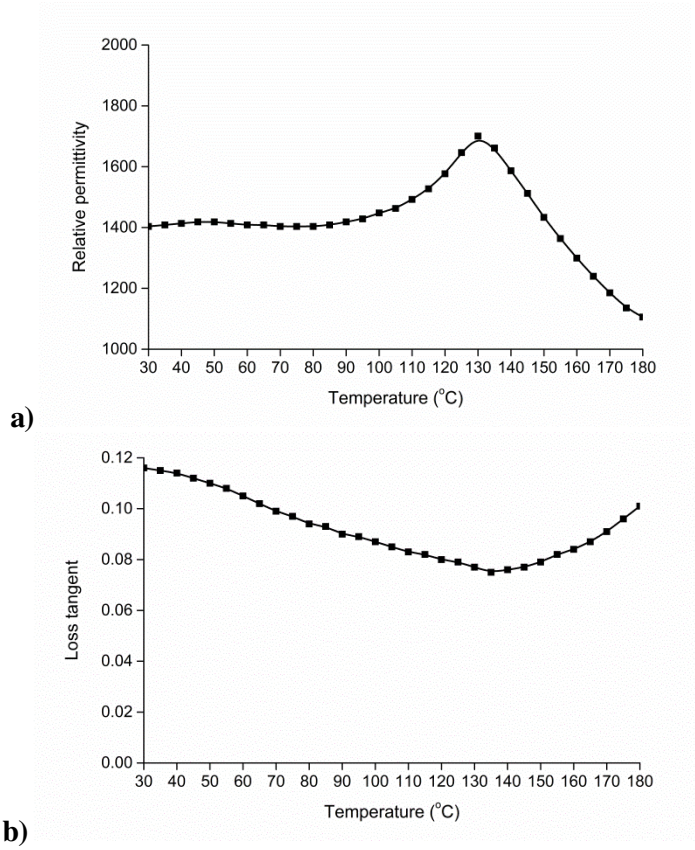

Fig. 5. a) Relative permittivity and b) loss tangent of BTF1300.

The broadening would be more significant if the iron oxide content was larger. The loss tangent is in the range 0.7-0.12, exhibiting its minimum of 0.7 near 130 °C. At the measurement frequency of 5MHz, the permittivity and loss tangent values are near their intrinsic values because the charge relaxation mechanisms are not active at this frequency. Previous studies of $BaTiO_3/Fe_2O_3$ composites reported dielectric permittivity between 65 and 600 with loss tangents between 0.05 and 0.2 in the temperature range 60-130 °C [31]. In our case, the composite obtained by *in situ* reaction had a significantly higher permittivity in the same temperature range due to the better homogeneity and more intimate contact between the phases, compared to other ferroelectric/magnetic composites [32-34].

4. Conclusion

In this paper, we have investigated a $BaTiO_3/\varepsilon\text{-}Fe_2O_3$ multiferroic composite and its behaviour at elevated temperatures. Nanocrystalline $\varepsilon\text{-}Fe_2O_3$ was obtained by a chemical route. The distribution of $\varepsilon\text{-}Fe_2O_3$ in the $BaTiO_3$ matrix was uniform, as confirmed by the SEM and EDS analyses. Sintering of the prepared composite was performed at 1300 °C for 1 h. The XRD revealed the heterostructured multiferroic composite comprising ferroelectric $BaTiO_3$ as the main phase along with the magnetic $BaFe_{12}O_{19}$ and $Ba_{12}Ti_{28}Fe_{15}O_{84}$ phases. The obtained composite shows a high value of the dielectric permittivity measured at 5 MHz, with the maximum of 1700 at the Currie temperature. The broadening of the permittivity maximum is correlated with the presence of various phases, both ferroelectric and magnetic.

Acknowledgments

Funds for the realization of this work were provided by the Ministry of Education, Science and Technological Development of the Republic of Serbia, Agreement on realization and financing of scientific research work of the Institute of Technical Sciences of SASA in 2020 (Record number: 451-03-68 / 2020-14 / 200175), and the project F133 funded by the Serbian Academy of Sciences and Arts.

This work was financially supported by the Serbian Ministry of Education, Science and Technological Development (Grant No. 451-03-68/2020-14/200026 and 451-03-68/2020-14/200288). This work is supported by NSF PREM award DMR 11523617.

5. References

1. N. Stojanović, A. Kalezić-Glišović, A. Janićijević, and A. Maričić, Science of Sintering 52, (2020).
2. R. M. Thankachan, B. Raneesh, A. Mayeen, S. Karthika, S. Vivek, S. S. Nair, S. Thomas, and N. Kalarikkal, Journal of Alloys and Compounds 731, 288 (2018).
3. O. Condurache, I. Turcan, L. Curecheriu, C. Ciomaga, P. Postolache, G. Ciobanu, and L. Mitoseriu, Ceramics International 43, 1098 (2017).
4. L. Loh, J. Briscoe, and S. Dunn, Nanoscale 6, 7072 (2014).
5. P. N. Oliveira, D. M. Silva, G. S. Dias, I. A. Santos, and L. F. Cótica, Ferroelectrics 499, 76 (2016).
6. Y. Cui, H. Sun, J. Briscoe, R. Wilson, N. Tarakina, S. Dunn, and Y. Pu, Nanotechnology 30, 255702 (2019).
7. A. Stajčić, I. Radović, V. Ćosović, A. Grujić, J. Stajić-Trošić, and R. Jančić-Heinemann, Science of Sintering 51, 277 (2019).
8. L. Curecheriu, P. Postolache, V. Buscaglia, N. Horchidan, M. Alexe, and L. Mitoseriu, Phase Transitions 86, 670 (2013).
9. G. Sreenivasulu, M. Popov, F. A. Chavez, S. L. Hamilton, P. R. Lehto, and G. Srinivasan, Appl. Phys. Lett. 104, 052901 (2014).
10. M. T. Buscaglia, V. Buscaglia, L. Curecheriu, P. Postolache, L. Mitoseriu, A. C. Ianculescu, B. S. Vasile, Z. Zhe, and P. Nanni, Chem. Mater. 22, 4740 (2010).
11. Y. S. Koo, K. M. Song, N. Hur, J. H. Jung, T.-H. Jang, H. J. Lee, T. Y. Koo, Y. H. Jeong, J. H. Cho, and Y. H. Jo, Appl. Phys. Lett. 94, 032903 (2009).
12. M. T. Buscaglia, V. Buscaglia, M. Viviani, P. Nanni, and M. Hanuskova, Journal of the European Ceramic Society 20, 1997 (2000).
13. M. B. Smith, K. Page, T. Siegrist, P. L. Redmond, E. C. Walter, R. Seshadri, L. E. Brus, and M. L. Steigerwald, J. Am. Chem. Soc. 130, 6955 (2008).
14. Y. Li, Z. Liao, F. Fang, X. Wang, L. Li, and J. Zhu, Appl. Phys. Lett. 105, 182901 (2014).
15. P. V. Balachandran, D. Xue, and T. Lookman, Phys. Rev. B 93, 144111 (2016).
16. S. Filipović, L. Anđelković, D. Jeremić, P. Vulić, A. S. Nikolić, S. Marković, V. Paunović, S. Lević, and V. B. Pavlović, Science of Sintering 52, (2020).
17. L. Shu, Z. Li, J. Ma, Y. Gao, L. Gu, Y. Shen, Y. Lin, and C. W. Nan, Appl. Phys. Lett. 100, 022405 (2012).
18. S. Filipović, V. P. Pavlović, M. Mitrić, S. Lević, N. Mitrović, A. Maričić, B. Vlahović, and V. B. Pavlović, J Adv Ceram 8, 133 (2019).
19. [19] S. Sakurai, A. Namai, K. Hashimoto, and S. Ohkoshi, https://doi.org/10.1021/ja9046069.
20. C. Marius and I. Grozescu, POLITEHNICA" Univ. (Timişoara) Volume 54, (2009).
21. K. Kelm and W. Mader, Zeitschrift Für Naturforschung B 61, (2006).

22. O. Malina, J. Tuček, P. Jakubec, J. Kašlík, I. Medřík, H. Tokoro, M. Yoshikiyo, A. Namai, S. Ohkoshi, and R. Zbořil, RSC Adv. 5, 49719 (2015).
23. R. G. McCLEAN, M. A. Schofield, W. F. Kean, C. V. Sommer, D. P. Robertson, D. Toth, and M. Gajdardziska-Josifovska, European Journal of Mineralogy 13, 1235 (2001).
24. D. A. Balaev, I. S. Poperechny, A. A. Krasikov, K. A. Shaikhutdinov, A. A. Dubrovskiy, S. I. Popkov, A. D. Balaev, S. S. Yakushkin, G. A. Bukhtiyarova, O. N. Martyanov, and Yu. L. Raikher, Journal of Applied Physics 117, 063908 (2015).
25. J. López-Sánchez, A. Muñoz-Noval, A. Serrano, M. Abuín, J. de la Figuera, J. F. Marco, L. Pérez, N. Carmona, and O. Rodríguez de la Fuente, RSC Adv. 6, 46380 (2016).
26. Y. Jiang, Z. Zhang, Z. Zhou, H. Yang, and Q. Zhang, Polymers 11, 1541 (2019).
27. https://www.rigaku.com/support/software/pdxl.
28. https://www.icdd.com/.
29. S. Filipović, N. Obradović, S. Marković, M. Mitrić, I. Balać, A. Đorđević, and V. Pavlović, Advanced Powder Technology 30, 2533 (2019).
30. J. A. Sans, V. Monteseguro, G. Garbarino, M. Gich, V. Cerantola, V. Cuartero, M. Monte, T. Irifune, A. Muñoz, and C. Popescu, Nature Communications 9, 4554 (2018).
31. L. Curecheriu, P. Postolache, M. T. Buscaglia, V. Buscaglia, A. Ianculescu, and L. Mitoseriu, Journal of Applied Physics 116, 084102 (2014).
32. R. Grigalaitis, M. M. Vijatović Petrović, J. D. Bobić, A. Dzunuzovic, R. Sobiestianskas, A. Brilingas, B. D. Stojanović, and J. Banys, Ceramics International 40, 6165 (2014).
33. B. Want, M. ud D. Rather, and R. Samad, J Mater Sci: Mater Electron 27, 5860 (2016).
34. S. Y. Tan, S. R. Shannigrahi, S. H. Tan, and F. E. H. Tay, Journal of Applied Physics 103, 094105 (2008).

Сажетак: *Реакцијом у чврстом стању између $BaTiO_3$ и Fe_2O_3 добијен је мултифероични хетероструктурни композит. Комерцијални $BaTiO_3$ и $Fe(NO_3)_3$•$9H_2O$ су помешани у етанолу 30 минута у ултразвучном купатилу. Припремљена смеша је термички обрађена на 300 °C 6 h. Синтеровање на 1300 °C у трајању од 1 h резултовало је формирањем вишефазног система, $BaTiO_3$, $BaFe_{12}O_{19}$ и $Ba_{12}Ti_{28}Fe_{15}O_{84}$, што је потврђено XRPD анализом. Густа микроструктура са затвореном порозношћу је потврђена скенирајућом електронском микроскопијом, док је мапирањем потврђена равномерна дистрибуција јона гвожђа преко фазе баријум титаната. Допирање $BaTiO_3$ са Fe_2O_3 резултовало је формирањем магнетних хексаферитних фаза, што је потврђено мерењем диелектричних параметара и ширењем максимума пермитивности мерене у функцији температуре.*

Кључне речи*:$BaTiO_3$, композити, мултифероик, реакција у чврстом стању, синтеровање.*